Molecular Biology of the Cell
Vol. 12, 3973–3986, December 2001

Dominant-Lethal α-Tubulin Mutants Defective in Microtubule Depolymerization in Yeast[V]

Kirk R. Anders and David Botstein*

Department of Genetics, Stanford University School of Medicine, Stanford, California 94305

Submitted September 5, 2001; Revised October 9, 2001; Accepted October 15, 2001
Monitoring Editor: J. Richard McIntosh

The dynamic instability of microtubules has long been understood to depend on the hydrolysis of GTP bound to β-tubulin, an event stimulated by polymerization and necessary for depolymerization. Crystallographic studies of tubulin show that GTP is bound by β-tubulin at the longitudinal dimer-dimer interface and contacts particular α-tubulin residues in the next dimer along the protofilament. This structural arrangement suggests that these contacts could account for assembly-stimulated GTP hydrolysis. As a test of this hypothesis, we examined, in yeast cells, the effect of mutating the α-tubulin residues predicted, on structural grounds, to be involved in GTPase activation. Mutation of these residues to alanine (i.e., D252A and E255A) created poisonous α-tubulins that caused lethality even as minor components of the α-tubulin pool. When the mutant α-tubulins were expressed from the galactose-inducible promoter of *GAL1*, cells rapidly acquired aberrant microtubule structures. Cytoplasmic microtubules were largely bundled, spindle assembly was inhibited, preexisting spindles failed to completely elongate, and occasional, stable microtubules were observed unattached to spindle pole bodies. Time-lapse microscopy showed that microtubule dynamics had ceased. Microtubules containing the mutant proteins did not depolymerize, even in the presence of nocodazole. These data support the view that α-tubulin is a GTPase-activating protein that acts, during microtubule polymerization, to stimulate GTP hydrolysis in β-tubulin and thereby account for the dynamic instability of microtubules.

INTRODUCTION

Microtubules are cytoskeletal structures that function in eukaryotes to segregate chromosomes during cell division, position organelles, organize the cytoplasm, and provide form and motility to cilia and flagella. A central property of microtubules is that they are dynamic; at steady state, individual microtubules can independently alternate between periods of stability (lengthening) and instability (shrinking) (Mitchison and Kirschner, 1984). This dynamic instability allows microtubules to probe efficiently intracellular space for targets such as chromosome kinetochores or polar cortical elements (Hayden *et al.*, 1990; Holy and Leibler, 1994; Carminati and Stearns, 1997; Shaw *et al.*, 1997), and microtubule assembly/disassembly is capable of providing motive force (reviewed by Inoue and Salmon, 1995). Although cellular factors modulate microtubule dynamics both spatially and temporally, the dynamic instability of microtubules results fundamentally from the properties of their component building blocks: α-β-tubulin heterodimers (Mitchison and Kirschner, 1984; reviewed by Desai and Mitchison, 1997).

Microtubules are polymers of α-β-tubulin heterodimers that align head to tail in linear protofilaments; 12–15 of these interact laterally to form a hollow tube (Nogales *et al.*, 1999). Microtubules grow by the addition of heterodimers containing GTP bound to β-tubulin, and this polymerization is accompanied by strong stimulation of the GTPase activity of β-tubulin (David-Pfeuty *et al.*, 1977; Caplow and Shanks, 1990; Desai and Mitchison, 1997). Experiments with the slowly hydrolyzable GTP analog GMPCPP demonstrate that nucleotide hydrolysis is a key event required for microtubule depolymerization, but it is not necessary for polymerization (Hyman *et al.*, 1992; Caplow *et al.*, 1994). The free energy released from nucleotide hydrolysis is largely stored as tension in the microtubule lattice, which is later released when protofilaments containing GDP-bound β-tubulin curl and peel away from the microtubule wall, driving depolymerization (Caplow *et al.*, 1994; Muller-Reichert *et al.*, 1998). To explain the temporary stability of a growing microtubule whose body is composed of heterodimers containing GDP-bound β-tubulin, a long-held model suggests that a cap of heterodimers containing GTP-bound β-tubulin at the growing end prevents disassembly and effectively traps the unstable GDP-containing heterodimers within the microtubule

[V] Online version of this article contains video material for certain figures. Online version available at www.molbiolcell.org.

* Corresponding author. E-mail address: botstein@genome.stanford.edu.

lattice (Mitchison and Kirschner, 1984; Desai and Mitchison, 1997).

How does microtubule polymerization stimulate the GTP hydrolysis that facilitates subsequent depolymerization? Crystallographic studies of tubulin show that the GTP bound by β-tubulin also contacts particular α-tubulin residues (D251 and E254) across the longitudinal dimer-dimer interface that is formed only when dimers are polymerized (Nogales *et al.*, 1998b, 1999). Erickson (1998) and Nogales *et al.* (1998a) suggest that α-tubulin might act as a GTPase-activating protein and, upon polymerization, might stimulate GTP hydrolysis through these contacts, particularly the γ-phosphate–interacting E254. Support for this hypothesis comes from studies of the tubulin-like protein FtsZ of bacteria, where mutation of D212 (the amino acid homologous to E254 of α-tubulin) inhibits GTP hydrolysis without significantly affecting GTP binding or FtsZ polymerization (Dai *et al.*, 1994; Mukherjee and Lutkenhaus, 1994; Trusca *et al.*, 1998). This hypothesis, however, has not been tested directly with tubulin. Here we examine, in living yeast cells, the effect of mutating these α-tubulin residues predicted to be involved in GTPase activation.

α-Tubulin is encoded by two genes in the yeast *Saccharomyces cerevisiae*, *TUB1* and *TUB3*. Tub1p constitutes the major fraction of the α-tubulin pool and Tub3p, 90% identical to Tub1p, contributes only a minor fraction of the α-tubulin (Schatz *et al.*, 1986a). Consequently, deletion of *TUB1* is lethal, whereas loss of *TUB3* results in viable cells that are supersensitive to the microtubule drug benomyl (Schatz *et al.*, 1986b). *TUB1* and *TUB3* are functionally interchangeable: each can compensate for the loss of the other when expressed at appropriate levels (Schatz *et al.*, 1986b).

As part of a systematic charged-to-alanine mutagenesis of *TUB1* (Richards *et al.*, 2000), the allele *TUB1-828* was obtained that consists of two changes in the amino acids predicted to be involved in GTPase activation: D252A and E255A (yeast α-tubulin amino acid residue numbers are +1 relative to those of the tubulin crystal structure, due to an additional amino acid at position 44). D252 is conserved in nearly all tubulins and in bacterial FtsZ (which is structurally nearly identical), whereas E255 is specific to α-tubulins (Nogales *et al.*, 1998a). The *TUB1-828* phenotype is dominant-lethal, although the lethality can be suppressed by increased dosage of the wild-type allele (Richards *et al.*, 2000). The dominance is particularly striking, considering that changing glutamate or aspartate to alanine is usually thought of as resulting in a *loss* of a potential binding or catalytic substituent. To determine the function of these α-tubulin residues, we studied the effect on microtubules caused by α-tubulins mutant for these residues. To do this, we transiently induced their expression in otherwise wild-type cells and observed the resulting phenotypes.

MATERIALS AND METHODS

Media and Genetic Manipulations

Standard methods were used for growth, sporulation, and genetic analysis of yeast (Guthrie and Fink, 1991), except for the following differences in media formulation: YEP was supplemented with 50 mg/l adenine sulfate; synthetic complete (SC) and drop-out media were supplemented with 40 mg/l L-alanine, 40 mg/l L-cysteine, 40 mg/l L-proline, and contained 50 mg/l adenine sulfate, 60 mg/l L-tyrosine, 80 mg/l L-isoleucine, and, if included, 100 mg/l L-leucine and 100 mg/l L-lysine. 5-Fluoroorotic acid (5-FOA) was used at 0.2%. Unless otherwise noted, carbon sources were supplemented to 2% (wt/vol) and cells were grown at 25°C in synthetic drop-out media to maintain plasmids. Benomyl, a gift from DuPont (Wilmington, DE), and nocodazole (Sigma, St. Louis, MO) were kept as 10 mg/ml stocks in dimethyl sulfoxide at −20°C. α-Factor (Sigma) was stored as a 5 mg/ml methanol stock at −20°C.

Construction of Plasmids

Plasmids are listed in Table 1. Oligonucleotides are listed in Table 2. Plasmids were constructed twice independently. All mutant alleles of *TUB1* and *TUB3* were confirmed by the presence of a new restriction site cogenerated with the mutation (Table 2). pRB2940 (*TUB1-D252A*) was generated by oligonucleotide-mediated mutagenesis of pRB2065 with the use of oligonucleotide 786 as described (Richards *et al.*, 2000). pRB2942 (*TUB1-E255A*) was constructed by with the use of oligonucleotide primer pairs 168/785 and 782/783 to amplify overlapping mutant *TUB1* fragments from pRB326 template DNA in a *Pfu* polymerase polymerase chain reaction (Stratagene, La Jolla, CA). These fragments were gel purified then used as templates for a second amplification with the use of primers 1068 and 1069 to generate a full-length fusion product. The 1.4-kb *Xho*I-*Msc* I fragment from this fusion product was cloned into the *Xho*I and *Msc* I sites of pRB2065, replacing a wild-type fragment of *TUB1*. pRB2945 (*TUB3*) was constructed by ligating the 3.3-kb *Bgl*II *TUB3* fragment from pRB300 into *Bam*HI of YIplac211 (which had its *Eco*RI site removed by cutting, filling-in with Klenow polymerase, and religating). pRB2947 (*TUB3-E255A*) was constructed by with the use of primer pairs 378/799, 798/480, and 479/480, and pRB300 as template in a fusion PCR scheme as described above to generate DNA containing an E255A mutation in *TUB3*. The 290-base pair *Eco*RI fragment from this fusion product was cloned into the *Eco*RI sites of pRB2945, replacing the wild-type fragment of *TUB3*. To construct pRB2785 and pRB2949-2958 (gal-inducible *tub1* alleles on *CEN* plasmid), *Pfu* polymerase (Stratagene) was used in PCRs to amplify *TUB1* from wild-type genomic DNA (DBY6600), *TUB1-828* from pRB2335, *TUB1-D252A* from pRB2940, *TUB1-E255A* from pRB2942, *TUB1-820* from pRB2311, and *tub1-827* from pRB2332 with the use of primers 781 and 782. The PCR products were digested with *Bam*HI and *Spe*I and ligated to the *Bam*HI and *Xba*I sites of pTS210. Digested PCR products from wild-type DNA and pRB2335 were ligated to pTS408 as described above to generate pRB2960 (*GAL1p-GFP::TUB1*) and pRB2963 (*GAL1p-GFP::TUB1-828*).

Construction of Yeast Strains

Yeast strains are listed in Table 3. *TUB1-D252A* and *TUB1-E255A* heterozygous strains DBY9557 and DBY9559 were constructed by one-step integration of pRB2940 and pRB2942 into DBY6596 as described (Richards *et al.*, 2000). Two independently derived plasmids were transformed for each allele to guard against misinterpretation of mutant phenotypes that might be due to unplanned mutations occurring during construction of the plasmids or the integrated yeast strains. Each independently constructed plasmid yielded indistinguishable dominant-lethal phenotypes.

To construct *TUB3-E255A* strains, DBY6597, containing pRB327 (*TUB1*), was transformed with *Xho*I-linearized pRB2947, integrating at *TUB3*. The extra plasmid-borne copies of *TUB1* were included to help avoid potential inviability or aneuploidy that results from certain α-tubulin mutations (Schatz *et al.*, 1986b; Richards *et al.*, 2000). Transformants were plated to 5-fluoroorotic acid to select for recombinational excision of the *URA3*-based plasmid then screened by PCR and *Mlu* I restriction digest to identify those derivatives that retained *TUB3-E255A* (DBY9563). DBY9563 was sporulated and *TUB3-E255A* haploids were identified by PCR as described above, as well as by their inability to

Table 1. Plasmids used in this study

Name	Description	Source or reference
pTS210	*CEN*-based vector with *GAL1-10* promoter and *ACT1* terminator	Marschall *et al.* (1996)
pTS408	*CEN*-based vector with GFP under *GAL1* promoter and *ACT1* terminator	Carminati and Stearns (1997)
pTS988	*GFP(S65T)*::*TUB1* integrative vector containing *LEU2*	T. Stearns (Stanford University)
YIplac211	Integrative vector containing *URA3*	Gietz and Sugino (1988)
pRB300	*TUB3* in pBR322-derived vector	Schatz *et al.* (1986b)
pRB326	*TUB1* in *CEN*-based vector containing *URA3*	Schatz *et al.* (1986b)
pRB327	*TUB1* in 2μ-based vector containing *LEU2*	Schatz *et al.* (1986b)
pRB2065	pUC119 vector containing *TUB1* marked with flanking *LEU2* integration	Richards *et al.* (2000)
pRB2311	pRB2065 containing *TUB1-820*	Richards *et al.* (2000)
pRB2332	pRB2065 containing *tub1-827*	Richards *et al.* (2000)
pRB2335	pRB2065 containing *TUB1-828*	Richards *et al.* (2000)
pRB2940	pRB2065 containing *TUB1-D252A*	This study
pRB2942	pRB2065 containing *TUB1-E255A*	This study
pRB2785	*TUB1* under *GAL1* promoter (*GAL1p-TUB1*)	This study
pRB2945	*TUB3* integrative vector containing *URA3*	This study
pRB2947	*TUB3-E255A* integrative vector containing *URA3*	This study
pRB2949	*TUB1-828* under *GAL1* promoter (*GAL1p-TUB1-828*)	This study
pRB2951	*TUB1-D252A* under *GAL1* promoter (*GAL1p-TUB1-D252A*)	This study
pRB2953	*TUB1-E255A* under *GAL1* promoter (*GAL1p-TUB1-E255A*)	This study
pRB2956	*TUB1-820* under *GAL1* promoter (*GAL1p-TUB1-820*)	This study
pRB2958	*tub1-827* under *GAL1* promoter (*GAL1p-tub1-827*)	This study
pRB2960	*GFP*::*TUB1* under *GAL1* promoter (*GAL1p-GFP*::*TUB1*)	This study
pRB2963	*GFP*::*TUB1-828* under *GAL1* promoter (*GAL1p-GFP*::*TUB1-828*)	This study
pRB2804	*GFP(S65T)*::*TUB1* under *ACT1* promoter in *CEN*-based plasmid containing *LEU2*	This laboratory

lose pRB327. A plasmid-shuffling scheme was used to replace pRB327 (*TUB1, LEU2*) with pRB2785 (*GAL1-TUB1, URA3*), followed by transformation with pRB2804 (*ACT1p-GFP::TUB1*) to generate DBY9574 and DBY9576.

Strains DBY9583–7 were constructed by transforming DBY6597 with pTS210, pRB2785, and pRB2949-53 then sporulating and dissecting to yield haploid spore clones. DBY9584-5 were transformed with pRB2804 to yield DBY9589-90.

To construct strains DBY9579-80, DBY8915 was transformed with *Xba*I-linearized pTS988 to integrate at *TUB1*. Transformants were screened by fluorescent microscopy to identify those (~50%) with green fluorescent protein (GFP)-labeled microtubules, which were backcrossed successively to FY2 and FY23 to yield progeny (including DBY9579 and DBY9580) that had wild-type growth phenotypes on glucose, galactose, and glycerol, in aerobic and anaerobic conditions, at various temperatures (11–37°C), and on media containing benomyl (5–30 μg/ml).

Table 2. Oligonucleotides used in this study

Uppercase letters indicate identity to wild-type sequence. Oligonucleotides 784 and 786 contain a codon 252 mutation (GAT^{Asp} to GCT^{Ala}) and a silent mutation at codon 248 (TCA^{Ser} to TCT^{Ser}) that creates a diagnostic *Dra*I site. Oligonucleotides 783, 785, 798, and 799 contain a mutation at codon 255 (GAA^{Glu} to GCG^{Ala}) that creates *Mlu*I and *Afl*III sites. Oligonucleotide 781 contains a *Bam*HI site. Oligonucleotide 782 contains a *Spe*I site. Oligonucleotides 479 and 480 contain a *Bam*HI site.

Oligonucleotide	Name	Sequence
168	TUB1-182U(+)	CACCGTAGTTTCCGGCCG
378	TUB3-172U	GAGCAGAGCATATCGTCC
479	KStub3-01	ccgccatggagATGAGAGAGGTCATTAGT
480	KStub3-02	gcgccatggTTAGAACTCCTCAGCGTA
781	KAtub1-01	cggggatccATGAGAGAAGTTATTAGTA
782	KAtub1-02	ggactagtAGAAAGGATAAGGAGGTTG
783	KAtub1-E255A	AATGTAGATTTGAACGcgTTTCAAACCAATTTGG
785	KAtub1-E255Arev	CCAAATTGGTTTGAAAcgCGTTCAAATCTACATT
784	KAtub1-D252A	GATTCGACGGTTCtTTAAATGTAGcTTTGAACGAATTTCAAAC
786	KAtub1-D252rev	GTTTGAAATTCGTTCAAAgCTACATTTAAaGAACCGTCGAATC
798	KAtub3E255A-F	AACGcgTTTCAGACCAACTTGGTA
799	KAtub3E255A-R	GTCTGAAAcgCGTTCAAATCCAC
1068	KAtub1-03	AATATCACCGTAGTTTCCGGC
1069	KAtub1-04	AGAAAGGATAAGGAGGTTGGG

Table 3. Yeast strains used in this study

Strain	Genotype	Source or reference
FY2	*MAT* **a** *ura3-52*	Winston *et al.* (1995)
FY23	*MAT* **a** *ura3-52 leu2-Δ1 trp1-Δ63*	Winston *et al.* (1995)
DBY2637	*MAT* **a** *his2-Δ200 leu2-3,112 lys2-801 ura3-52 tub1Δ::HIS3 tub3Δ::TRP1* [pRB327]	This laboratory
DBY6596	*MAT* **a**/α *ade2-101/ade2-101 his3-Δ200/his3-Δ200 lys2-801/lys2-801 leu2-Δ1/leu2-Δ1 ura3-52/ura3-52 TUB1–LEU2/tub1Δ::HIS3* [pRB326]	Richards *et al.* (2000)
DBY6597	*MAT* **a**/α *ade2-101/ade2-101 his3-Δ200/his3-Δ200 lys2-801/lys2-801 leu2-Δ1/leu2-Δ1 ura3-52/ura3-52 [pRB326]*	This laboratory
DBY6600	*MAT* **a**/α *ade2-101/ade2-101 his3-Δ200/his3-Δ200 lys2-801/lys2-801 leu2-Δ1/leu2-Δ1 ura3-52/ura3-52 TUB1–LEU2/TUB1–LYS2* [pRB326]	Richards *et al.* (2000)
DBY6627	*MAT* **a**/α *ade2-101/ade2-101 his3-Δ200/his3-Δ200 lys2-801/lys2-801 leu2-Δ1/leu2-Δ1 ura3-52/ura3-52 tub1-827–LEU2/TUB1–LYS2* [pRB326]	Richards *et al.* (2000)
DBY6628	*MAT* **a**/α *ade2-101/ade2-101 his3-Δ200/his3-Δ200 lys2-801/lys2-801 leu2-Δ1/leu2-Δ1 ura3-52/ura3-52 TUB1-828–LEU2/TUB1–LYS2* [pRB326]	Richards *et al.* (2000)
DBY8247	*MAT* **a**/α *ade2-101/ade2-101 his3-Δ200/his3-Δ200 lys2-801/lys2-801 leu2-Δ1/leu2-Δ1 ura3-52/ura3-52 TUB1-820–LEU2/TUB1–LYS2* [pRB326]	Richards *et al.* (2000)
DBY8915	*MAT* **a** *ade2-(ΔEcoRV - Stu1) lys2-ΔEcoRV leu2-Δ1 ura3-52*	This laboratory
DBY9557	*MAT* **a**/α *ade2-101/ade2-101 his3-Δ200/his3-Δ200 lys2-801/lys2-801 leu2-Δ1/leu2-Δ1 ura3-52/ura3-52 TUB1-D252A–LEU2/TUB1–LYS2* [pRB326]	This study
DBY9559	*MAT* **a**/α *ade2-101/ade2-101 his3-Δ200/his3-Δ200 lys2-801/lys2-801 leu2-Δ1/leu2-Δ1 ura3-52/ura3-52 TUB1-E255A–LEU2/TUB1–LYS2* [pRB326]	This study
DBY9561	*MAT* **a** *his2-Δ200 leu2-3,112 lys2-801 ura3-52 tub1Δ::HIS3 tub3Δ::TRP1* [pRB2785]	This study
DBY9562	*MAT* **a** *his2-Δ200 leu2-3,112 lys2-801 ura3-52 tub1Δ::HIS3 tub3Δ::TRP1* [pRB326]	This study
DBY9563	*MAT* **a**/α *ade2-101/ade2-101 his3-Δ200/his3-Δ200 lys2-801/lys2-801 leu2-Δ1/leu2-Δ1 ura3-52/ura3-52 TUB3-E255A/TUB3* [pRB327]	This study
DBY9565	*MAT* **a**/α *ade2-101/ade2-101 his3-Δ200/his3-Δ200 lys2-801/lys2-801 leu2-Δ1/leu2-Δ1 ura3-52/ura3-52 TUB3-E255A/TUB3* [pRB2785]	This study
DBY9566	*MAT* **a**/α *ade2-101/ade2-101 his3-Δ200/his3-Δ200 lys2-801/lys2-801 leu2-Δ1/leu2-Δ1 ura3-52/ura3-52 TUB3/TUB3* [pRB2785]	This study
DBY9574	*MAT* **a** *ade2-101 his3-Δ200 lys2-801 leu2-Δ1 ura3-52 TUB3* [pRB2785, pRB2804]	This study
DBY9576	*MAT* **a** *ade2-101 his3-Δ200 lys2-801 leu2-Δ1 ura3-52 TUB3-E255A* [pRB2785, pRB2804]	This study
DBY9578	*MAT* **a**/α *ade2-101/ade2-101 his3-Δ200/his3-Δ200 lys2-801/lys2-801 leu2-Δ1/leu2-Δ1 ura3-52/ura3-52 TUB3-E255A/TUB3* [pRB326]	This study
DBY9579	*MAT* **a** *ade2-(ΔEcoRV - Stu1) leu2-Δ1 ura3-52*	This study
DBY9580	*MAT* **a** *ade2-(ΔEcoRV - Stu1) leu2-Δ1 ura3-52 GFP(S65T)::TUB1–LEU2*	This study
DBY9583	*MAT* **a** *ade2-101 his3-Δ200 lys2-801 leu2-Δ1 ura3-52* [pTS210]	This study
DBY9584	*MAT* **a** *ade2-101 his3-Δ200 lys2-801 leu2-Δ1 ura3-52* [pRB2785]	This study
DBY9585	*MAT* **a** *ade2-101 his3-Δ200 lys2-801 leu2-Δ1 ura3-52* [pRB2949]	This study
DBY9586	*MAT* **a** *ade2-101 his3-Δ200 lys2-801 leu2-Δ1 ura3-52* [pRB2960]	This study
DBY9587	*MAT* **a** *ade2-101 his3-Δ200 lys2-801 leu2-Δ1 ura3-52* [pRB2963]	This study
DBY9589	*MAT* **a** *ade2-101 his3-Δ200 lys2-801 leu2-Δ1 ura3-52* [pRB2785, pRB2804]	This study
DBY9590	*MAT* **a** *ade2-101 his3-Δ200 lys2-801 leu2-Δ1 ura3-52* [pRB2949, pRB2804]	This study

Cell Cycle Synchronizations

Cells were grown in raffinose medium to 1–5 × 10^6 cells/ml. α-Factor was added to 2.5 μM and cells were incubated for 2.25–3 h, resulting in >93% unbudded cells. For galactose induction during α-factor–induced arrest, galactose was added and cells were incubated 2 h. A portion of the culture was either fixed for antibody staining or directly examined for GFP staining. The remainder of the cells was washed into glucose medium and incubated until removed for examination. For galactose induction during hydroxyurea-induced arrest, α-factor–arrested cells were washed into raffinose medium containing freshly dissolved 0.1 M hydroxyurea and incubated for 2.5 h, resulting in >90% budded cells. Galactose was added to the culture and incubated for 2 h. The cells were washed into glucose medium containing 2.5 μM α-factor to prevent a second budding after cytokinesis. Aliquots were removed every 30 min and killed with sodium azide, lightly sonicated, and fixed for staining with 4′,6′-diamidino-2-phenylindole (Rose *et al.*, 1990), or were examined directly for GFP staining.

Viability Assays

Cells were grown exponentially in medium containing 2% raffinose to a density of 1–5 × 10^6 cells/ml. At time zero, galactose was added to the culture to 2%. At each time point, cells were removed from liquid culture, lightly sonicated, diluted into glucose medium, and plated. Sonication was with the Heat Systems-Ultrasonics (Misonix, Farmingdale, NY) W-225 sonicator with microtip, output control 5, 0.5–1 s in 0.3–0.5-ml volume. At the same time, an aliquot of cells was killed with sodium azide (20–33 μM), lightly sonicated, and cell density was determined either by hemacytometer or by the Beck-

man Coulter Z2 particle counter (Beckman Coulter, Fullerton, CA). Viability was determined by the number of colonies formed in 3–5 d/100 cells plated.

Microscopy

To visualize microtubules by immunofluorescence, cells were fixed in 3.7% formaldehyde, stained with the anti-α-tubulin antibody YOL1/34 (Accurate Chemical & Scientific, Westbury, NY), and images obtained with an Olympus microscope equipped with a Photometrix PXL cooled charge-coupled device camera as described by Schwartz *et al.* (1997).

To visualize GFP-labeled microtubules, 1–2 μl of cells was placed on a 1% agarose pad containing growth medium. Images were obtained with a Zeiss Axioskop microscope (Carl Zeiss, Thornwood, NY) equipped with a Pan-Neofluar 100×/0.7–1.3 adjustable aperture oil immersion objective lens, an HBO 100W mercury lamp, the 41017 Endow GFP bandpass filter set (Chroma, Brattleboro, VT), Uniblitz lamp shutters (Vincent Associates, Rochester, NY), and a Hamamatsu 4742-95 ORCA-100 charge-coupled device camera (Hamamatsu Photonics, Hamamatu City, Japan). The camera and shutters were controlled with SimplePCI imaging software (version 3.0; Compix, Cranberry Township, PA). To obtain time-lapse series, the excitation light was attenuated by 75% with a neutral density filter, and the images were captured once every 10–20 s with a 0.5–1-s exposure. Microtubule lengths were measured with the use of SimplePCI to determine the length, in pixels, of a line manually drawn along the length of a microtubule. Pixel size was correlated to physical distance by measuring the diameters of 3.0-μm Monosized Polymer Microspheres (Duke Scientific, Palo Alto, CA), resulting in a metric of 17.9 pixels/μm. For microtubules partly out of the plane of focus but still visible, an estimated length was determined. To estimate rate of microtubule growth and shrinkage, a regression line and coefficient of determination were calculated by linear least squares.

RESULTS

α-Tubulins Containing Mutations D252A and/or E255A Are Potent Poisons

The dominant-lethal α-tubulin allele *TUB1-828* encodes alanines in place of the residues aspartate-252 and glutamate-255 (D252A and E255A), which are located at the longitudinal interdimer interface that is created when heterodimers are polymerized in a protofilament (Richards *et al.*, 2000; Figure 1A). A strain heterozygous for *TUB1-828* that contains extra plasmid-borne copies of *TUB1* is viable, but does not survive when loss of the plasmid is selected for by 5-FOA (Figure 2A). To determine whether the dominant lethality of *TUB1-828* is specific to one of the two mutated residues, we constructed heterozygous *TUB1* mutants containing either D252A or E255A (*TUB1-D252A* and *TUB1-E255A*) as described in MATERIALS AND METHODS. These mutants were also inviable on 5-FOA, indicating that they are also dosage dependent, dominant-lethal alleles (Figure 2A). We infer that when half of the Tub1p in the cell (the major α-tubulin component) contains D252A and/or E252A mutations, the cell cannot survive.

To determine whether a smaller fraction of α-tubulin would cause lethality, we constructed the E255A mutation in *TUB3*. The heterozygote *TUB3-E255A/TUB3*, containing extra plasmid-borne *TUB1*, was also inviable on 5-FOA (Figure 2A). To generate a strain in which the extra *TUB1* expression could be repressed in all cells simultaneously, a plasmid containing *TUB1* under the control of the galactose-inducible and glucose-repressible promoter of the *GAL1* gene was placed in a *TUB3-E255A/TUB3* mutant. The resulting strain was viable when grown on galactose, but was inviable on glucose, a condition where the extra *TUB1* expression is repressed (Figure 2B). We conclude that E255A-mutant α-tubulin is a lethal poison even when it constitutes only half of the minor α-tubulin component (Tub3p) of the cell.

To control the expression of the dominant-lethal α-tubulin alleles, they were placed downstream of the *GAL1* promoter

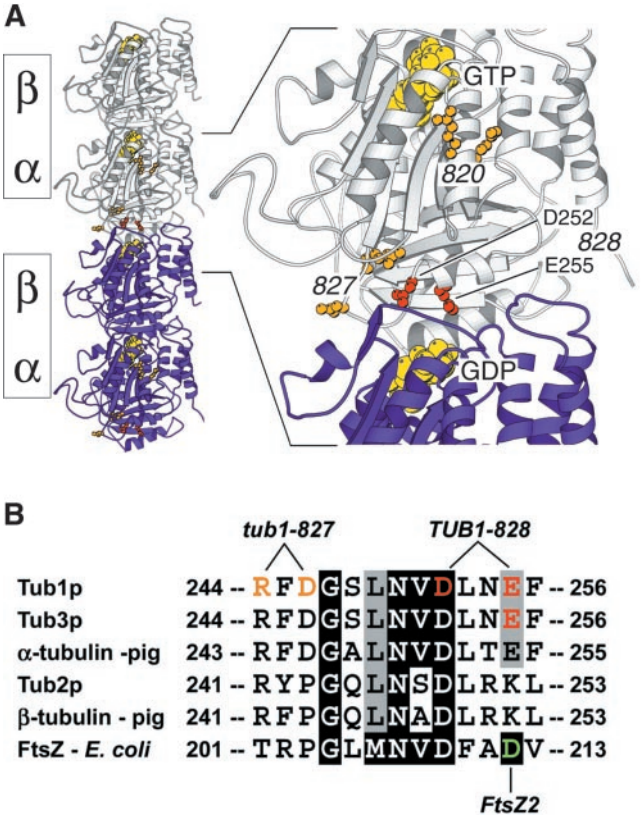

Figure 1. Location of α-tubulin mutations in this study. (A) Two α-β dimers longitudinally aligned in a protofilament show the location of yeast α-tubulin mutations relative to the interdimer interface. The structure shown is bovine tubulin (Nogales *et al.*, 1998b) with amino acid side chains drawn that correspond to those identical residues mutated in the following *S. cerevisiae* alleles: *TUB1-820* (E156A, E157A) and *tub1-827* (R244A, D246A) shown in orange, and *TUB1-828* (D252A, E255A) (Richards *et al.*, 2000), *TUB1-D252A*, *TUB1-E255A*, and *TUB3-E255A* shown in red. Structure is oriented with the plus end up and the outside face of the microtubule to the right. Guanine nucleotides are shown in yellow. Structure drawn with Molscript (Kraulis, 1991). (B) Alignment of α-tubulin, β-tubulin, and FtsZ sequences in the region of longitudinal interaction. Residues shared by the tubulins and FtsZ are shaded. Residues mutated in the yeast tubulin alleles described in A are orange or red. The residue mutated in the GTPase-defective allele *ftsZ2* (D212G) is green (Dai *et al.*, 1994). Amino acid sequences (Swiss-Prot ID: TUBA1_YEAST, TUBA3_YEAST, TBA_PIG, TBB_YEAST, TBB_PIG, FTSZ_ECOLI) were aligned with Clustal W (Thompson *et al.*, 1994). Because bovine tubulin sequence is unknown, porcine tubulin sequence is applied to the bovine crystal structure (Nogales *et al.*, 1998b).

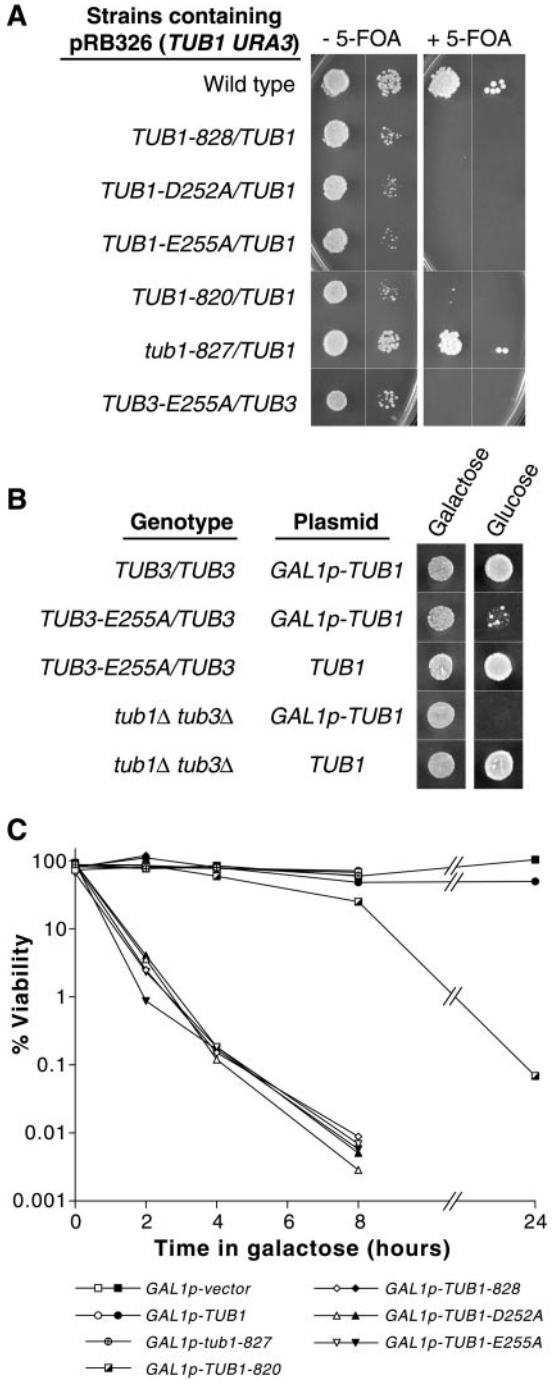

Figure 2. Dosage-dependent, dominant lethality of α-tubulin alleles containing D252A and/or E255A mutations. (A) Extra copies of *TUB1* confer viability to dominant-lethal α-tubulin alleles. Strains containing pRB326 (*TUB1*, *URA3*) plasmid were grown overnight in liquid medium supplemented with uracil to allow the loss of the plasmid then spotted to plates containing 5-FOA to select for Ura(−) cells that had lost the plasmid. Approximately 10^4 and 10^2 cells were spotted to SC-lys,-leu,-ura without 5-FOA (SC-ura for *TUB3-E255A/TUB3*) and to SC supplemented with 5-FOA and grown for 3 d. Strains shown are DBY6600, DBY6628, DBY9557, DBY9559, DBY8247, DBY6627, and DBY9578. (B) *TUB3-E255A/TUB3* strain is on centromeric plasmids and transformed into wild-type strain DBY9579. The resulting strains had wild-type growth rates on glucose or raffinose but were inviable on galactose. In galactose, cells rapidly lost viability (ca. 100-fold in one generation time; Figure 2C). Similarly expressed wild-type *TUB1*, *tub1-827* (another interdimer interface mutant allele) and *TUB1-820* (a dominant-lethal allele affecting another part of the molecule) caused little lethality in the same time frame. These results were recapitulated in the independently derived diploid strain DBY6597 and its haploid progeny DBY9583-5 (Figure 6A), indicating that the observed lethality is not strain dependent. We conclude that transient expression of α-tubulin that contains D252A and/or E255A mutations causes fatal damage that persists even after the expression of the mutant tubulin is repressed.

Expression of α-Tubulins Containing Mutations D252A and/or E255A Results in Aberrant Microtubule Structures

To visualize microtubules in the mutant cells, strain DBY9580 was constructed by integrating an extra copy of *TUB1* fused to the GFP into the *TUB1* locus. This strain, derived from the same tetrad as DBY9579 (see above), behaved like wild-type under many growth conditions, including temperatures between 11 and 37°C, different carbon sources, and benomyl-containing media, and the dominant-lethal α-tubulin phenotypes remained unchanged (Figure 2C). After 2-h exposure to galactose, cells expressing any of the dominant-lethal *GAL1*-driven *TUB1* alleles contained aberrant microtubule structures (Figure 3A). Cytoplasmic microtubules were largely bundled, with occasional individual microtubules observed. Long, late-anaphase spindles were absent, but shorter spindles were observed, often with less intense fluorescence at their centers. A small fraction of the cells (<5%) contained microtubules that appeared unattached to spindle pole bodies (Figures 3B and 8B). Expression of *TUB1-D252A* consistently resulted in microtubules that were shorter than those of *TUB1-828* or *-E255A*. Time-lapse photomicroscopy revealed that the bundled microtubules originated both from cells in G1 and from cells that underwent anaphase with incomplete spindle elongation (Figure 3B). These phenotypes were not artifacts due to *GFP::TUB1*, because cells lacking the fusion protein exhibited the same aberrant microtubule structures when fixed and stained with anti-tubulin antibodies (Figure 5D).

Figure 2. {cont). inviable when ectopic *GAL1p-TUB1* expression is repressed by glucose. Strains containing pRB2785 (*GAL1p-TUB1*) or pRB326 (*TUB1*) plasmids were grown overnight in galactose-containing medium then ~10^4 cells were spotted to SC-ura plates containing galactose or glucose and grown for 3 d. Strains shown are DBY9566, DBY9565, DBY9578, DBY9561, and DBY9562. (C) Viability after transient expression of plasmid-borne *GAL1p-TUB1* alleles. Raffinose-containing cultures were treated with galactose to induce expression of *GAL1p-TUB1* alleles then plated to glucose-containing plates to repress *GAL1p-TUB1* allele expression. Viability is expressed in percentage of cells plated that resulted in colonies. Open symbols indicate that strain DBY9579 contains the designated plasmid. Black- and pattern-filled symbols indicate that strain DBY9580 (with a *GFP::TUB1-LEU2* insertion), contains the designated plasmid.

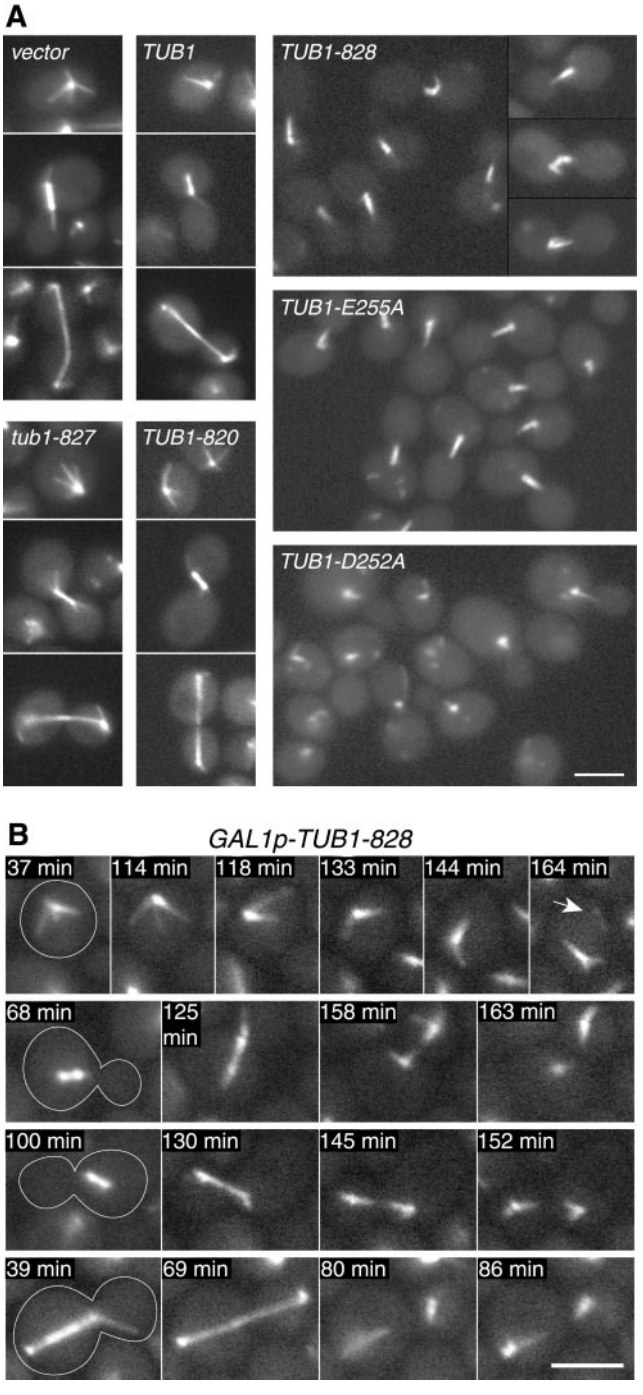

Figure 3. Morphology of the microtubule cytoskeleton after expression of mutant *GAL1p-TUB1* alleles. (A) GFP-labeled microtubules in cells exposed to galactose for 2 h then washed into glucose medium and incubated 1 h. Cells are strain DBY9580 containing one of the following plasmids, pTS210 (*GAL1p-vector*), pRB2785 (*GAL1p-TUB1*), pRB2956 (*GAL1p-TUB1-820*), pRB2958 (*GAL1p-tub1-827*), pRB2949 (*GAL1p-TUB1-828*), pRB2953 (*GAL1p-TUB1-E255A*), or pRB2951 (*GAL1p-TUB1-D252A*). [Nonmicrotubular spots of GFP fluorescence are occasionally seen with all plasmids except *GAL1p-vector*, similar to those described by Carminati and Stearns (1997).] (B) Time-lapse series showing the appearance of aberrant microtubule morphologies upon expression of *GAL1p-TUB1-828*. Galactose (2%) and glucose (0.2%) were added to a raffinose culture of strain DBY9580 + pRB2949 (*GAL1p-TUB1-828*) at time zero. Cells were mounted onto a microscope slide containing 2% galactose, 0.2% glucose medium and GFP fluorescence was visualized every 20 s. Arrow indicates loose microtubule that became unattached to the spindle pole body. **Videos 3B_1.mov, 3B_2.mov, 3B_3.mov, and 3B_4.mov** contain entire series from 30 to 164 min of galactose exposure. Bars, 3 μm.

GFP::Tub1-828p Can Be Incorporated into Microtubules

To determine whether Tub1-828p can be incorporated into growing microtubules, we expressed a GFP::Tub1-828p fusion protein by galactose induction. Expression of *GFP::TUB1-828* caused inviability and microtubule defects with similar kinetics as described above for *TUB1-828* (Figure 4A). Visualization studies showed that GFP::Tub1-828p was incorporated into the lengths of both nuclear spindle microtubules and cytoplasmic microtubules (Figure 4B). In contrast to the wild-type GFP::Tub1p, GFP::Tub1-828p provided a relatively bright signal at the spindle pole bodies. We infer from these results that α-tubulin containing D252A and E255A mutations is competent to be assembled into microtubules.

TUB1-828 Expression Inhibits Normal Spindle Assembly

Because few spindles appeared normal after *TUB1-828* expression, we were interested in determining whether spindles could assemble in the presence of Tub1-828p. We induced *TUB1-828* expression in cells that were blocked at a stage of the cell cycle before spindle assembly then released the cells to proceed through the cell cycle. Cells were arrested in G1 with the mating pheromone α-factor then exposed to galactose for 2 h to induce *TUB1-828* expression. The cells were released from the pheromone block by washing into glucose medium, allowing the cell cycle to proceed. After 90 min, ~65% of the cells that carried control plasmid containing *GAL1*-driven *TUB1* or the *GAL1* promoter alone had normal-looking assembled spindles, whereas only 8% of cells containing *GAL1*-driven *TUB1-828* contained normal-appearing spindles (Figure 5, B and C). Rather, most *TUB1-828*--expressing cells contained aberrant bundles of microtubules, indicating that normal spindles did not assemble properly.

Surprisingly, many of the cells expressing the mutant α-tubulin contained microtubules that were not attached to the presumed spindle pole body, both before and after release from α-factor (Figure 5, A and B, arrows). These unattached microtubules were localized predominantly to the schmoo extension or the subsequent bud. There was a lower prevalence of unattached microtubules after release from α-factor, suggesting that their formation was largely during the mating pheromone-induced arrest and that they were eventually depolymerized. Such unattached microtubules also appeared in fixed and immunostained cells, indicating that their origin did not depend on *GFP::TUB1* or the conditions under which the live cells were placed during microtubule visualization.

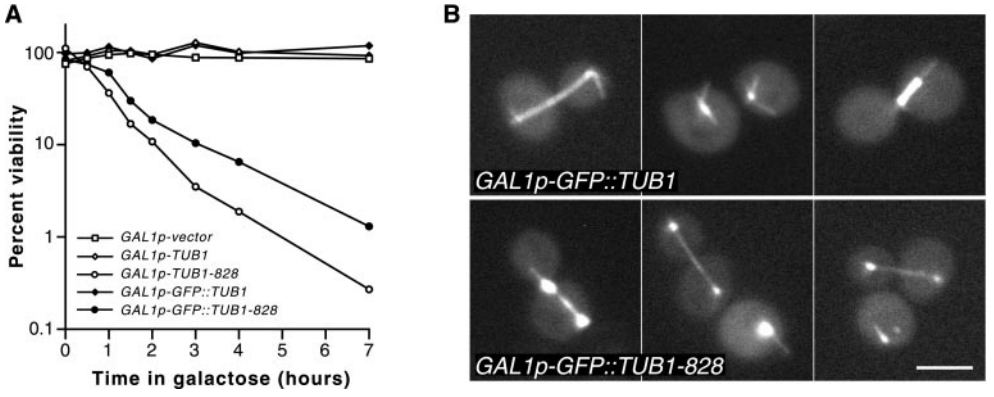

Figure 4. Cell viability and microtubule structures after expression of *GFP::TUB1-828* and *GFP::TUB1*. (A) Viability after transient expression of *GAL1*-driven *TUB1* alleles. Raffinose cultures were treated with galactose then plated to glucose-containing plates. Viability is expressed in percentage of cells plated that resulted in colonies. Strain is DBY6597 containing pTS210 (*GAL1p-vector*), pRB2785 (*GAL1p-TUB1*), pRB2949 (*GAL1p-TUB1-828*), pRB2960 (*GAL1p-GFP::TUB1*), and pRB2963 (*GAL1p-GFP::TUB1-828*). (B) GFP-labeled microtubules after galactose-in-duction of *GFP::TUB1* and *GFP::TUB1-828* expression. Haploid spore clones from A (strains DBY9586-7) were grown in raffinose then treated with 2% galactose, 0.2% glucose for 3.5 h. Bar, 3 μm.

TUB1-828 Expression Inhibits Spindle Elongation and Maintenance of Spindle Structure

To determine the effect of Tub1-828p on spindles once they are assembled, we performed a cell cycle block experiment similar to that described above: we expressed *TUB1-828* in arrested cells containing assembled, pre-anaphase spindles then released the cells from the cell cycle block. Cells were first synchronized with α-factor (to increase the efficiency of the later block) then released into medium containing hydroxyurea, which causes an S-phase arrest with large buds and pre-anaphase spindles (Byers and Goetsch, 1974). After 2.5 h, the cultures contained >80% budded cells. Galactose was added to the medium and the cells were incubated an additional 2 h before they were released from hydroxyurea-induced arrest into glucose medium. Control cells that contained *GAL1*-driven *TUB1* or the empty vector then proceeded through the cell cycle normally, undergoing mitosis and cytokinesis 90–180 min after release from hydroxyurea. In contrast, most of the cells containing *GAL1*-driven *TUB1-828* failed to divide their nucleus or undergo cytokinesis (Figure 6A). When examined 120 min after release from hydroxyurea (Figure 6B), many of these cells contained aberrant spindle structures, with reduced GFP signal at their centers (arrows), and bundled cytoplasmic microtubules (arrowheads). Cells in which the spindle poles had separated contained small microtubule bundles similar to those seen in previous experiments (Figure 3B). We conclude that Tub1-828p interferes with the maintenance of the spindle structure after spindle assembly, and prevents proper spindle elongation.

TUB1-828 Expression Stops Microtubule Dynamics

To observe the effect of Tub1-828p on the dynamics of individual microtubules, *TUB1-828* expression was induced for 1.75 h, after which fluorescent microscopy images were obtained at 10-s intervals. Microtubule life-history graphs of representative cells are shown in Figure 7 (the underlying movies are provided in the electronic version). Whereas microtubules remained dynamic in the control strains carrying plasmid containing *GAL1*-driven *TUB1* or the *GAL1* promoter alone, microtubules in cells containing *GAL1*-driven *TUB1-828* changed very little in length during the course of observation. We infer that incorporation of Tub1-828p into the microtubules inhibits their depolymerization, because many microtubules could be followed for 5–10 min with minimal shortening, whereas individual wild-type microtubules grow and shrink visibly within a few minutes at most.

TUB1-828 Expression Results in Microtubules That Fail to Shrink in Nocodazole

To test this inference more directly, we used the well-characterized antimicrotubule drug nocodazole. In wild-type yeast cells, nocodazole induces rapid net depolymerization of microtubules; first, the more dynamic cytoplasmic microtubules disappear, followed by the less dynamic intranuclear spindle microtubules (Jacobs *et al.*, 1988). We compared the stability of microtubules in cells by inducing cells containing *GAL1*-driven tubulin constructs for 2.5 h and then placing the cells onto an agarose pad containing glucose medium and 15 μg/ml nocodazole. Microtubules in cells expressing *GAL1p-TUB1* depolymerized within seconds and failed to repolymerize (Figure 8A). In contrast, microtubules in cells expressing *TUB1-828* remained the same length for the entire 3 min of the time-lapse series. After 20 min on the nocodazole-containing medium, cytoplasmic microtubules were completely absent from the strain containing *TUB1*, and only spots (presumably at spindle pole bodies) and an occasional spindle remained (Figure 8B). In the strain expressing *TUB1-828*, nearly 80% of the cells contained microtubule-containing structures, both typical bundles and individual microtubules. In experiments where nocodazole was added in liquid culture for an hour, results were similar. We conclude that microtubules that contain Tub1-828p are substantially defective in depolymerization.

TUB3-E255A Cells Accumulate Nondynamic Microtubules after GAL1-Shutoff of Extra TUB1 Expression

In the experiments described above, the ratio of mutant to wild-type α-tubulin was increased and microtubules were drastically effected. This was achieved by increasing the expression of the mutant α-tubulin. An alternative means of

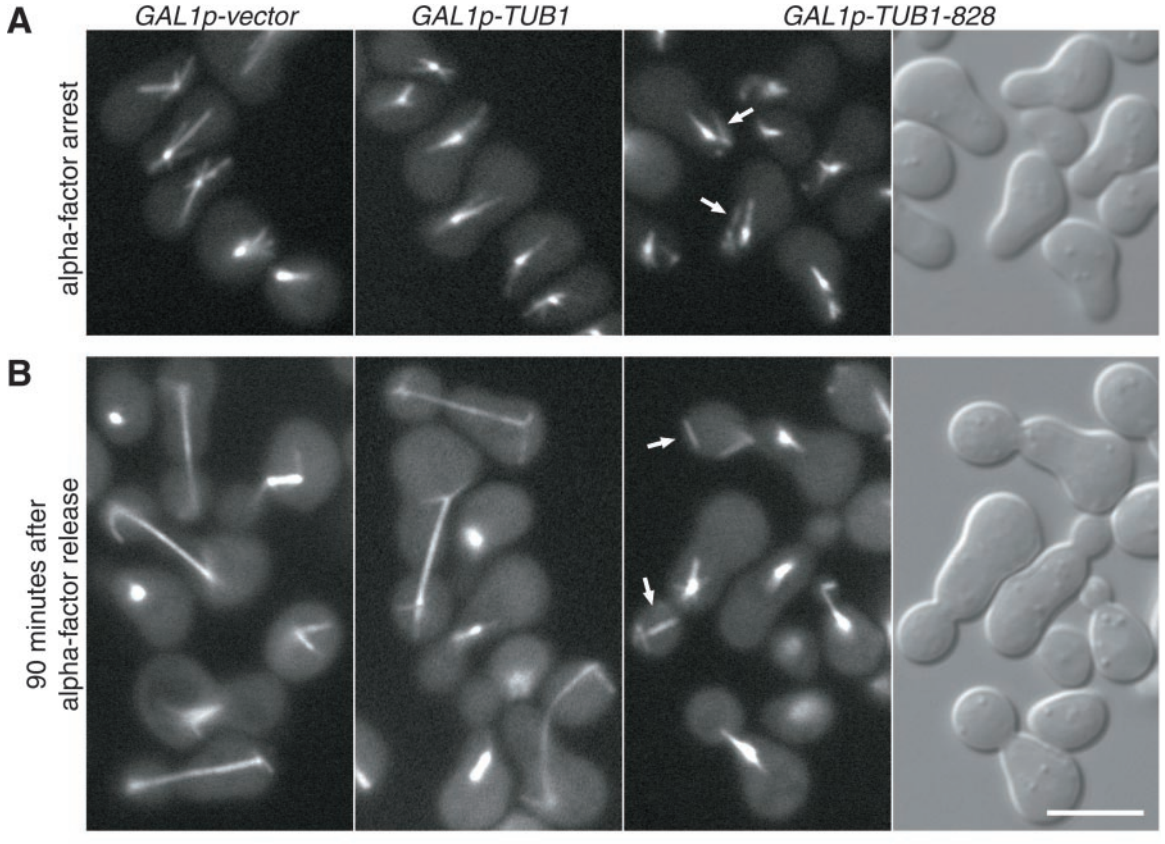

C

Percent of culture

GAL1p-vector n = 148	34	7	24	14	21	0	0	0	0
GAL1p-TUB1 n = 76	36	9	20	4	32	0	0	0	0
GAL1p-TUB1-828 n = 203	3	1	4	1	13	32	41	2	3

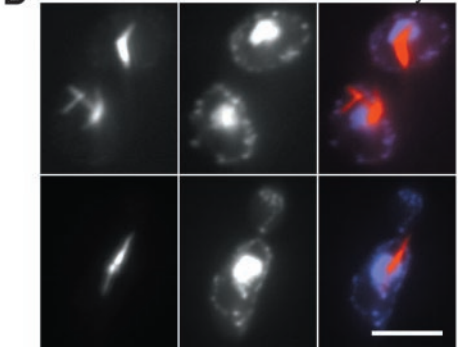

Figure 5. Expression of *TUB1-828* during G1 α-factor arrest results in unattached microtubules and inhibited spindle assembly upon release from α-factor arrest. (A and B) GFP-labeled microtubules in strain DBY9580, containing either pTS210 (*GAL1p-vector*), pRB2785 (*GAL1p-TUB1*), or pRB2949 (*GAL1p-TUB1-828*, also shown with differential interference contrast), grown in raffinose and arrested with α-factor then subjected to galactose for 2 h. In B, cells were released from α-factor arrest by washing into glucose medium and incubated for 90 min. Arrows indicate free microtubules not attached to the presumed spindle pole body. **Videos 5A_TUB1.mov** (*GAL1p-TUB1*) **and 5A_828.mov** (*GAL1p-TUB1-828*) illustrate microtubule dynamics under these conditions and movement of the free microtubules in A, 5B_828.mov (*GAL1p-TUB1-828*) shows cells in B. Bar, 5 μm. (C) Distribution of microtubule structures and cell shapes in cultures 90 min after release from α-factor arrest shown in B. Drawings above each column indicate presence of bud and appearance of microtubules. Aberrant microtubule bundles and unattached microtubules indicated in the four columns on the right. (D) Anti-tubulin antibodies reveal unattached microtubules and aberrant microtubule bundles in cells expressing *TUB1-828* in the absence of *GFP::TUB1*. Strain DBY9585, containing plasmid pRB2949 (*GAL1p-TUB1-828*), was arrested with α-factor in raffinose, subjected to galactose for 2 h (top row) then washed into galactose medium and grown for 3.5 h (bottom row). Control strains DBY9583 and DBY9584, containing plasmids pTS210 (*GAL1p-vector*) and pRB2785 (*GAL1p-TUB1*), appeared normal as in A and B (our unpublished data). Bar, 3 μm.

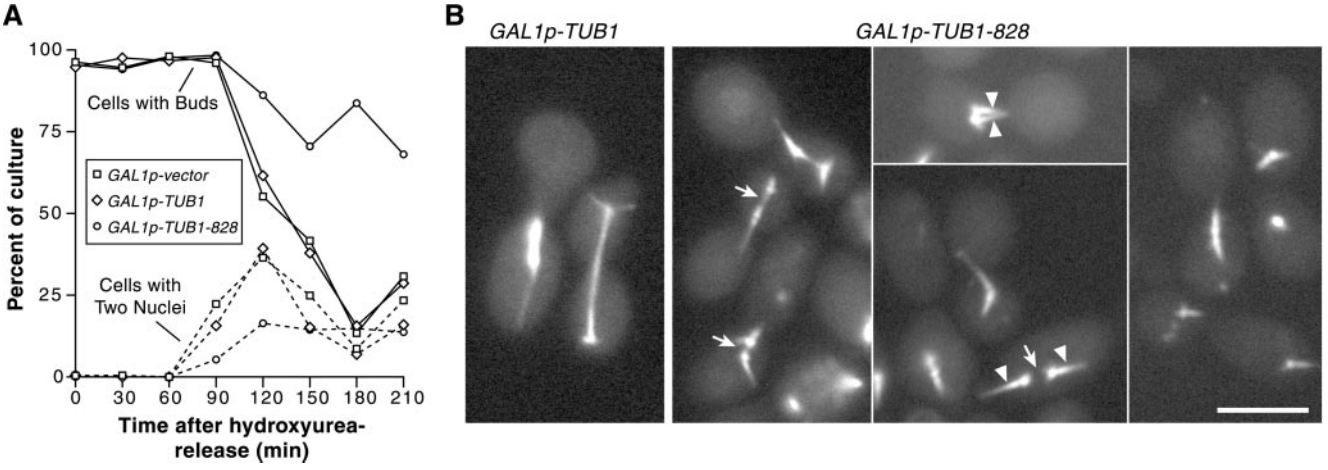

Figure 6. Expression of *TUB1-828* after spindles have assembled disrupts spindle integrity and inhibits normal spindle elongation. Strain DBY9580, containing either pTS210 (*GAL1p-vector*), pRB2785 (*GAL1p-TUB1*), or pRB2949 (*GAL1p-TUB1-828*), was released from G1 α-factor arrest into medium containing hydroxyurea for 2.5 h. Galactose was added and the cells incubated for 2 h. Cells were then released from hydroxyurea-induced arrest into glucose medium at time zero. α-Factor was included to prevent a second cell division. (A) Cell cycle progression after release from hydroxyurea-induced arrest. Numbers of nuclei were determined by 4′,6′-diamidino-2-phenylindole staining and fluorescence microscopy. At least 100 cells were counted for each time point. (B) GFP-labeled microtubules 90–120 min after release from hydroxyurea. Arrows indicate thinning or disappearance of intranuclear microtubules that span the distance between spindle pole bodies; arrowheads indicate bundled cytoplasmic microtubules. Bar, 3 μm.

increasing the ratio of mutant to wild-type α-tubulin, without overexpressing a mutant tubulin, is to reduce the quantity of wild-type α-tubulin. To accomplish this, we used a haploid strain that contains the chromosomal alleles *TUB3-E255A* and wild-type *TUB1*, a plasmid-borne *GAL1*-driven wild-type *TUB1* allele and, to visualize microtubules in live cells, a second plasmid containing the constitutively expressed *ACT1* promoter-driven *GFP::TUB1* (Figure 9A). This strain was viable when grown in galactose because the extra *TUB1* expression suppresses the dominant lethality of *TUB3-E255A*. However, this strain was inviable on glucose plates, producing only microcolonies consistent with approximately four cell doublings occurring before a complete arrest in cell division. As shown in Figure 9B, shift to glucose of this strain for 8 h (2 cell generations) resulted in microtubule phenotypes similar to those seen above, including large-budded cells with no spindle, loose microtubules; bright GFP staining of spindle pole bodies; and slower, less dynamic microtubules.

DISCUSSION

When α-β-tubulin heterodimers join head to tail to form protofilaments during microtubule polymerization, a longitudinal dimer-dimer interface is formed, which, according to the atomic model of the tubulin protofilament (Nogales *et al.*, 1998a), brings particular α-tubulin residues (D251 and E254) into proximity with the guanine nucleotide of β-tubulin (Figure 1). To investigate the function of these α-tubulin residues, we studied dominant-lethal mutants in which alanines had been substituted at these positions in the *S. cerevisiae* α-tubulins Tub1p and Tub3p. (The reader will recall that D251 and E254 are numbered D252 and E255 in yeast α-tubulins, and we will hereafter refer to them as D252 and E255.) To study the phenotypes in greater detail, we used two methods to change the ratio of mutant α-tubulin to wild-type α-tubulin so that cells would transition from unaffected to affected. One strategy involved overproduction of the mutant protein through use of the *GAL1* promoter, and the other used shut-off of transcription from the same promoter to decrease the level of wild-type α-tubulin. Together, these experiments revealed that expression of the dominant-lethal α-tubulin alleles interfered with microtubule dynamics.

It is worth reviewing the evidence that the significant defect is in depolymerization. First, assembly of GFP-tagged Tub1-828p into microtubules showed that α-tubulins containing D252A and E255A mutations are competent to participate in polymerization (Figure 4). Second, cells expressing TUB1-828 contained stable, long-lasting microtubules that did not depolymerize, even in the presence of nocodazole (Figures 7 and 8).

As indicated above, these data can be taken as strongly supporting the idea that α-tubulins containing D252A and E255A mutations inhibit microtubule dynamics directly by assembling into the growing polymer. We favor this direct mechanism over alternatives, which we cannot rule out completely, that suppose that the mutant α-tubulins, acting indirectly and/or outside of the microtubule lattice, block microtubule dynamics by interfering with other cellular factors that promote tubulin polymerization and depolymerization such as Bim1p, Bik1p, Stu2p, and the kinesin-related Kip3p and Kar3p (Cottingham *et al.*, 1999; Tirnauer *et al.*, 1999; Severin *et al.*, 2001; reviewed by Schuyler and Pellman, 2001).

The direct model we support envisions that α-tubulin is a GTPase-activating protein, and that this activity is eliminated or diminished when D252 and E255 are replaced by alanines. When heterodimers containing mutant α-tubulin

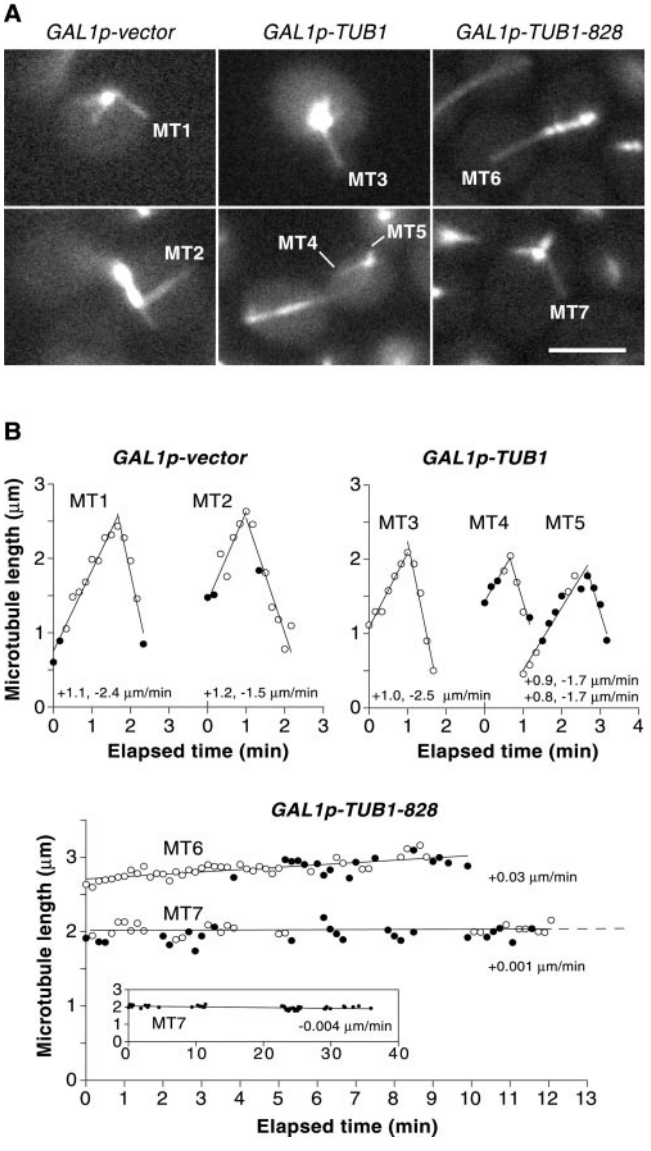

Figure 7. Time-lapse imaging showing the dynamics of GFP-labeled microtubules. Strain DBY9580, containing either pTS210 (*GAL1p-vector*), pRB2785 (*GAL1p-TUB1*), or pRB2949 (*GAL1p-TUB1-828*), was grown in raffinose medium then supplemented with 2% galactose, 0.2% glucose for 1.75 h and imaged within 1 h (*GAL1p-TUB1-828*) or within 2 h as described in MATERIALS AND METHODS. (A) Still frames from time-lapse series, supplied as **videos 7A_MT1.mov, 7A_MT2.mov, 7A_MT3.mov, 7A_MT4-5.mov, 7A_MT6.mov, and 7A_MT7.mov**. Black frames in the long-term series indicate removal of nonfocused images. Bar, 3 μm. (B) Graphs showing microtubule length over time for the individual microtubules (MT1-MT7) labeled in A. Open circles indicate microtubules in the focal plane, and filled circles indicate a microtubule partially out of the focal plane. A best-fit line was drawn for each growth and shrinkage phase, and its slope is indicated below each plot. Inset graph indicates the length of microtubule MT7 during 36 min of observation.

incorporate into the plus ends of growing microtubules (along with wild-type heterodimers), normal-appearing dimer-dimer interfaces can be formed between previously incorporated β-tubulin bound to GTP and mutant α-tubulin, but the concomitant stimulation of GTP hydrolysis in that adjacent β-tubulin is absent or strongly attenuated. Under this model, microtubule growth does not immediately cease, because GTP hydrolysis is not required for polymerization (Hyman *et al.*, 1992). If and when depolymerization is initiated somewhere above the mutant dimer, heterodimers containing GTP bound to β-tubulin are encountered and depolymerization halts. Although this is not an essential feature of our model, our data suggest further that repolymerization from the halted end is somehow difficult.

The central idea of this model is that α-tubulin is a GTPase-activating protein. Nogales *et al.* (1998a) and Erickson (1998) had suggested that the α-tubulin amino acids that were mutated in this study are positioned in such a way as to be able to stimulate the intrinsic GTPase of β-tubulin upon polymerization (Figure 1A). Furthermore, they noted that this idea would account nicely for the well-documented coincidence of GTP hydrolysis and polymerization. The tubulin crystal structure directly identifies D252 and E255 as α-tubulin residues that make close contacts with the β- and γ-phosphates of the guanine nucleotide at the dimer-dimer interface (Nogales *et al.*, 1998a, 1999). Although D252 is conserved across nearly all tubulins, E255 is conserved specifically in α-tubulins. The identical position in β-tubulin, located at the intradimer interface with α-tubulin and its (never hydrolyzed) GTP, is a specifically conserved lysine (Figure 1B). Finally, in the tubulin-like bacterial protein FtsZ, a mutation of the residue at the structurally conserved position of α-tubulin E255 (D212) inhibits GTP hydrolysis but not GTP binding (Dai *et al.*, 1994; Mukherjee and Lutkenhaus, 1994; Trusca *et al.*, 1998).

One of the strongest arguments for our model is that it accounts for dominant lethality caused by loss of a charged substituent, suggesting a loss of an interaction. When microtubules polymerize in the absence of guanine nucleotide hydrolysis, such as in experiments with the use of the slowly hydrolyzable GTP analog GMPCPP, microtubules are blocked in their ability to depolymerize (Hyman *et al.*, 1992; Caplow *et al.*, 1994). The dominant-lethal mutants we describe here have a phenotype entirely consistent with failure to stimulate GTP hydrolysis in β-tubulin. With this view, the mutations indeed result in loss of function (GTPase activation) that nevertheless display dominant phenotypes (loss of dynamic instability and lethality) at the cellular level.

It is not apparent from the current tubulin structure at 3.7-angstrom resolution how the removal of these residues would alter the GTPase active site of polymerized tubulin. Although there is a clear analogy at the level of function, there is no obvious structural similarity between α-tubulin and the classical Ras- and Rho-GTPase-activating proteins. The residues we studied in α-tubulin are negatively charged (aspartate and glutamate), whereas in the Ras-GTPase-activating proteins the catalysis is thought to involve an "arginine finger" (Nogales *et al.*, 1998a). We cannot distinguish between the nonexclusive possibilities that mutation of the negatively charged D252 and E255 residues directly removes a component required for GTP hydrolysis in the adjacent β-tubulin, or whether it causes a distortion of the interface structure that prevents the hydrolysis of GTP.

Our results are also consistent with other hypotheses that do not require the blocking of assembly-dependent GTP

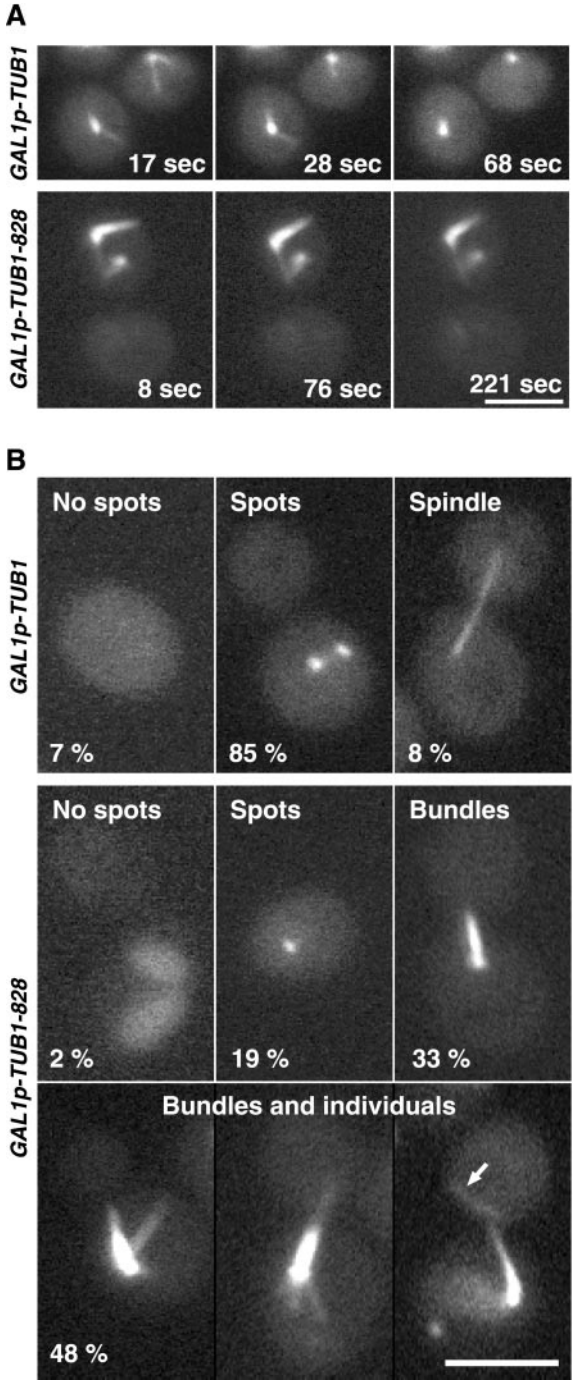

Figure 8. Effect of nocodazole in cells expressing *TUB1-828*. Strains DBY9589 (*GAL1p-TUB1*) and DBY9590 (*GAL1p-TUB1-828*) were exposed to galactose for 2.5 h then placed onto a glucose medium containing 15 μg/ml nocodazole. (A) Visualization of GFP-labeled microtubules after placement of cells onto nocodazole. Time-lapse series are available in **videos 8A_TUB1.mov (*GAL1p-TUB1*) and 8A_828.mov (*GAL1p-TUB1-828*).** (B) Microtubule structures after 20-min exposure to nocodazole. Percentage of culture is indicated for each morphological class. At least 100 cells were counted for each strain. Arrow indicates microtubule unattached to spindle pole body. Bars, 3 μm.

hydrolysis. If D252 and E255 are important for key conformational changes (induced by GTP hydrolysis) that promote depolymerization then perhaps microtubules are stabilized in our experiments despite normal GTP hydrolysis. Taxol, for example, stabilizes microtubules while still allowing GTP hydrolysis to occur (Schiff and Horwitz, 1981).

Our model suggests that depolymerizing microtubules become unable to transition back to polymerizing microtubules. Very few long microtubules were observed in cells expressing D252A- and E255A-mutant α-tubulins, and there appeared, when the mutants were expressed, to be a lot of tubulin fluorescence near spindle pole bodies, suggesting the existence of many short microtubules that could not be individually resolved (Figures 3, 6, and 9). Furthermore, when GFP::Tub1-828p was expressed, spindle-pole proximal GFP signal was predominant, again suggestive of many short microtubules (Figure 4). Spindles were not able to elongate and were blocked in full elongation of interpolar spindle microtubules during anaphase B (Figure 6).

Why might polymerization be inhibited in these mutants? It is possible that this is a secondary consequence of blocked depolymerization, perhaps because the pool of free dimers is already incorporated into the stable microtubules found in the bundles and near the spindle pole bodies. Alternatively, the fine structure of the microtubule ends may be "damaged" from defective depolymerization and may be unable to provide a proper template for polymerization phase of microtubule growth. Cryoelectron microscopic studies of the structure of microtubule ends indicate that depolymerizing microtubules appear to have a "fountain" of curving protofilaments that peel away from the wall of the microtubule, whereas microtubules likely in growth phase have either flush ends or open sheets that close together into a tube further away from the end (Mandelkow *et al.*, 1991; Chretien *et al.*, 1995; Muller-Reichert *et al.*, 1998; Arnal *et al.*, 2000). If, in the course of mutant microtubule depolymerization, some protofilaments peel away from the microtubule and others do not, or do so without depolymerizing, an end structure might result that cannot transition back into a growing end.

One surprising observation in the course of this study was the striking presence of loose, apparently detached, microtubules in cells that had expressed *TUB1-828* during α-factor arrest (Figure 5A). Mating pheromone causes a number of microtubule-related changes in cells, including increased expression of the kinesin Kar3p and a shift in the attachment of microtubules from the central outer plaque of the spindle pole body to the half-bridge (Byers and Goetsch, 1975; Meluh and Rose, 1990; Pereira *et al.*, 1999). Although we have no further evidence, it seems possible that either *TUB1-828* expression affects the integrity of microtubule attachment in pheromone, or that the abnormal stabilization of the microtubules has allowed the visualization of structures that normally occur but whose lifetime is normally cut short by depolymerization.

To conclude, we found that mutation of two charged α-tubulin residues predicted, on structural grounds, to be involved in activation of the β-tubulin GTPase, results in the formation of microtubules that have lost their dynamic instability in the living cell. Considering that the only charged-to-alanine mutations of α-tubulin with this kind of phenotype occur in this vicinity, and that the dominant-lethal

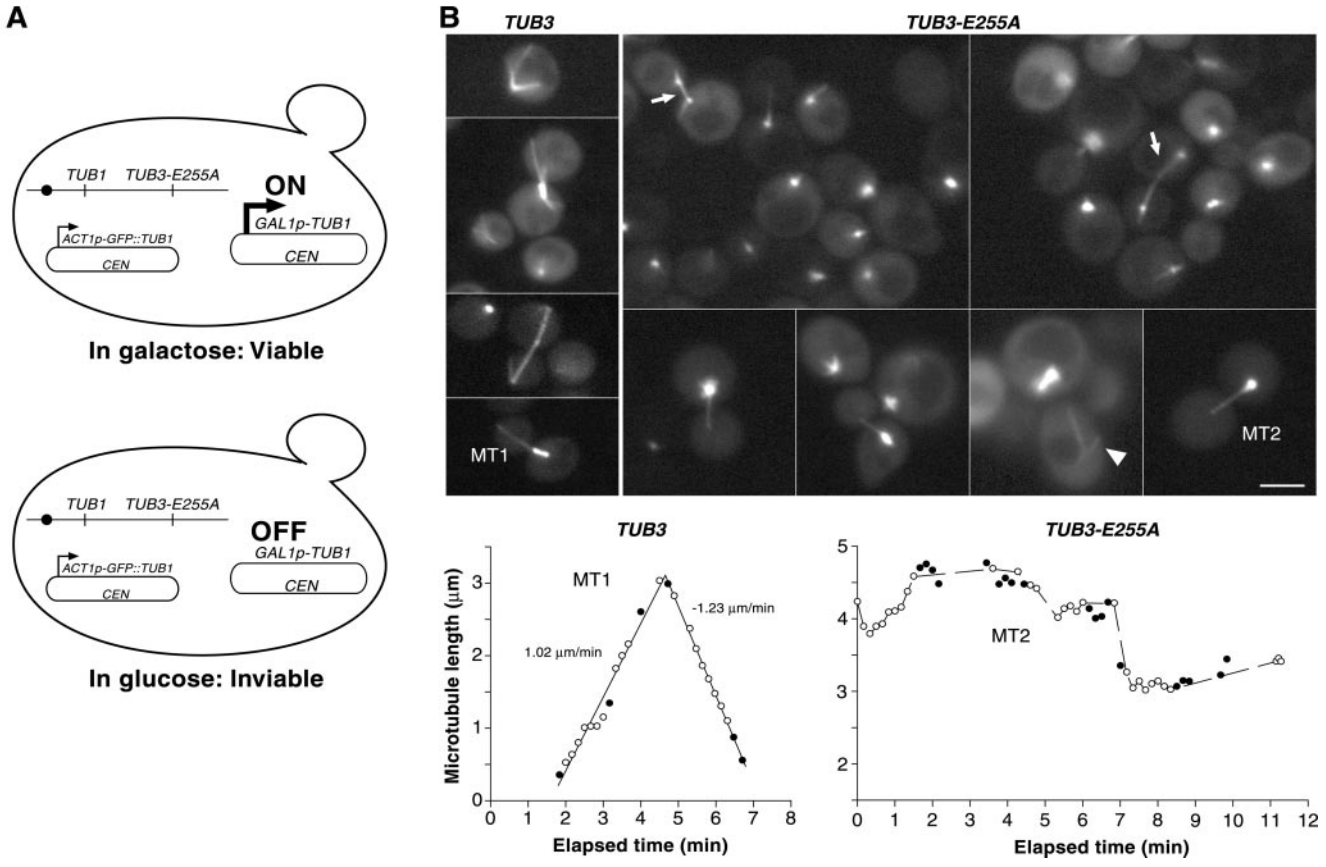

Figure 9. Visualization of the effect of *TUB3-E255A* on microtubules after *GAL1*-shutoff of ectopic *TUB1* expression. (A) Experimental scheme. Strain DBY9576, containing the lethal allele *TUB3-E255A*, is viable in galactose medium because suppressing quantities of wild-type *TUB1* are expressed from the *GAL1* promoter. When placed in glucose medium, transcription of the *GAL1p-TUB1* copy is repressed, and the cells become inviable. A copy of *GFP::TUB1* allows visualization of the microtubules. Strain DBY9574, which contains *TUB3*, serves as a control. (B) Microtubules in *TUB3* and *TUB3-E255A* strains after 8 h of glucose repression of *GAL1*-driven *TUB1*. Time-lapse series showing the dynamics of the representative microtubules MT1 and MT2 are contained in the **videos 9B_MT1.mov and 9B_MT2.mov**. Microtubule lengths are plotted over time. Open circles indicate microtubules in the focal plane, and filled circles indicate a microtubule partially out of the focal plane. For MT2 plot, dotted line connects in-focus data points. Arrows indicate anaphase spindles with poles brighter than along length, and arrowhead indicates unattached microtubule. Bar, 3 μm.

nature of these mutations inhibits, if not totally precludes, biochemical studies in vitro, this is probably as strong evidence for the hypothesized GTPase-activation function of α-tubulin as is possible to obtain at this time.

ACKNOWLEDGMENTS

We thank Eva Nogales and Ken Downing for fruitful discussions and for sharing data before publication, Tim Stearns and Katja Schwartz (Stanford University) for plasmids, and Jeff Dahlseid for critical reading of the manuscript. This work was supported by National Institutes of Health grant GM-46406 (to D.B.) and a National Institutes of Health Postdoctoral Fellowship (to K.A.).

REFERENCES

Arnal, I., Karsenti, E., and Hyman, A.A. (2000). Structural transitions at microtubule ends correlate with their dynamic properties in *Xenopus* egg extracts. J. Cell Biol. *149*, 767–774.

Byers, B., and Goetsch, L. (1974). Duplication of spindle plaques and integration of the yeast cell cycle. Cold Spring Harb. Symp. Quant. Biol. *38*, 123–131.

Byers, B., and Goetsch, L. (1975). Behavior of spindles and spindle plaques in the cell cycle and conjugation of *Saccharomyces cerevisiae*. J. Bacteriol. *124*, 511–523.

Caplow, M., Ruhlen, R.L., and Shanks, J. (1994). The free energy for hydrolysis of a microtubule-bound nucleotide triphosphate is near zero: all of the free energy for hydrolysis is stored in the microtubule lattice. J. Cell Biol. *127*, 779–788.

Caplow, M., and Shanks, J. (1990). Mechanism of the microtubule GTPase reaction. J. Biol. Chem. *265*, 8935–8941.

Carminati, J.L., and Stearns, T. (1997). Microtubules orient the mitotic spindle in yeast through dynein-dependent interactions with the cell cortex. J. Cell Biol. *138*, 629–641.

Cottingham, F.R., Gheber, L., Miller, D.L., and Hoyt, M.A. (1999). Novel roles for *Saccharomyces cerevisiae* mitotic spindle motors. J. Cell Biol. *147*, 335–350.

Chretien, D., Fuller, S.D., and Karsenti, E. (1995). Structure of growing microtubule ends: two-dimensional sheets close into tubes at variable rates. J. Cell Biol. *129*, 1311–1328.

Dai, K., Mukherjee, A., Xu, Y., and Lutkenhaus, J. (1994). Mutations in *ftsZ* that confer resistance to SulA affect the interaction of FtsZ with GTP. J. Bacteriol. *176*, 130–136.

David-Pfeuty, T., Erickson, H.P., and Pantaloni, D. (1977). Guanosinetriphosphatase activity of tubulin associated with microtubule assembly. Proc. Natl. Acad. Sci. USA *74*, 5372–5376.

Desai, A., and Mitchison, T.J. (1997). Microtubule polymerization dynamics. Annu. Rev. Cell Dev. Biol. *13*, 83–117.

Erickson, H.P. (1998). Atomic structures of tubulin and FtsZ. Trends Cell Biol. *8*, 133–137.

Gietz, R.D., and Sugino, A. (1988). New yeast-*Escherichia coli* shuttle vectors constructed with in vitro mutagenized yeast genes lacking six-base pair restriction sites. Gene *74*, 527–534.

Guthrie, C., and Fink, G.R. (1991). Guide to Yeast Genetics and Molecular Biology. Methods in Enzymology, vol. 194, San Diego: Academic Press.

Hayden, J.H., Bowser, S.S., and Rieder, C.L. (1990). Kinetochores capture astral microtubules during chromosome attachment to the mitotic spindle: direct visualization in live newt lung cells. J. Cell Biol. *111*, 1039–1045.

Holy, T.E., and Leibler, S. (1994). Dynamic instability of microtubules as an efficient way to search in space. Proc. Natl. Acad. Sci. USA *91*, 5682–5685.

Hyman, A.A., Salser, S., Drechsel, D.N., Unwin, N., and Mitchison, T.J. (1992). Role of GTP hydrolysis in microtubule dynamics: information from a slowly hydrolyzable analogue, GMPCPP. Mol. Biol. Cell *3*, 1155–1167.

Inoue, S., and Salmon, E.D. (1995). Force generation by microtubule assembly/disassembly in mitosis and related movements. Mol. Biol. Cell *6*, 1619–1640.

Jacobs, C.W., Adams, A.E., Szaniszlo, P.J., and Pringle, J.R. (1988). Functions of microtubules in the *Saccharomyces cerevisiae* cell cycle. J. Cell Biol. *107*, 1409–1426.

Kraulis, P.J. (1991). MOLSCRIPT: a program to produce both detailed and schematic plots of protein structures. J. Appl. Crystallogr. *24*, 946–950.

Mandelkow, E.M., Mandelkow, E., and Milligan, R.A. (1991). Microtubule dynamics and microtubule caps: a time-resolved cryo-electron microscopy study. J. Cell Biol. *114*, 977–991.

Marschall, L.G., Jeng, R.L., Mulholland, J., and Stearns, T. (1996). Analysis of Tub4p, a yeast gamma-tubulin-like protein: implications for microtubule-organizing center function. J. Cell Biol. *134*, 443–454.

Meluh, P.B., and Rose, M.D. (1990). KAR3, a kinesin-related gene required for yeast nuclear fusion. Cell *60*, 1029–1041.

Mitchison, T., and Kirschner, M. (1984). Dynamic instability of microtubule growth. Nature *312*, 237–242.

Mukherjee, A., and Lutkenhaus, J. (1994). Guanine nucleotide-dependent assembly of FtsZ into filaments. J. Bacteriol. *176*, 2754–2758.

Muller-Reichert, T., Chretien, D., Severin, F., and Hyman, A.A. (1998). Structural changes at microtubule ends accompanying GTP hydrolysis: information from a slowly hydrolyzable analogue of GTP, guanylyl (alpha, beta)methylenediphosphonate. Proc. Natl. Acad. Sci. USA *95*, 3661–3666.

Nogales, E., Downing, K.H., Amos, L.A., and Lowe, J. (1998a). Tubulin and FtsZ form a distinct family of GTPases. Nat. Struct. Biol. *5*, 451–458.

Nogales, E., Whittaker, M., Milligan, R.A., and Downing, K.H. (1999). High-resolution model of the microtubule. Cell *96*, 79–88.

Nogales, E., Wolf, S.G., and Downing, K.H. (1998b). Structure of the alpha beta tubulin dimer by electron crystallography. Nature *391*, 199–203.

Pereira, G., Grueneberg, U., Knop, M., and Schiebel, E. (1999). Interaction of the yeast gamma-tubulin complex-binding protein Spc72p with Kar1p is essential for microtubule function during karyogamy. EMBO J. *18*, 4180–4195.

Richards, K.L., Anders, K.R., Nogales, E., Schwartz, K., Downing, K.H., and Botstein, D. (2000). Structure-function relationships in yeast tubulins. Mol. Biol. Cell *11*, 1887–1903.

Rose, D., Thomas, W., and Holm, C. (1990). Segregation of recombined chromosomes in meiosis I requires DNA topoisomerase II. Cell *60*, 1009–1017.

Schatz, P.J., Pillus, L., Grisafi, P., Solomon, F., and Botstein, D. (1986a). Two functional alpha-tubulin genes of the yeast *Saccharomyces cerevisiae* encode divergent proteins. Mol. Cell. Biol. *6*, 3711–3721.

Schatz, P.J., Solomon, F., and Botstein, D. (1986b). Genetically essential and nonessential alpha-tubulin genes specify functionally interchangeable proteins. Mol. Cell. Biol. *6*, 3722–3733.

Schiff, P.B., and Horwitz, S.B. (1981). Taxol assembles tubulin in the absence of exogenous guanosine 5′-triphosphate or microtubule-associated proteins. Biochemistry *20*, 3247–3252.

Schuyler, S.C., and Pellman, D. (2001). Microtubule. "plus-end-tracking proteins": the end is just the beginning. Cell *105*, 421–424.

Schwartz, K., Richards, K., and Botstein, D. (1997). *BIM1* encodes a microtubule-binding protein in yeast. Mol. Biol. Cell *8*, 2677–2691.

Severin, F., Habermann, B., Huffaker, T., and Hyman, T. (2001). Stu2 promotes mitotic spindle elongation in anaphase. J. Cell Biol. *153*, 435–442.

Shaw, S.L., Yeh, E., Maddox, P., Salmon, E.D., and Bloom, K. (1997). Astral microtubule dynamics in yeast: a microtubule-based searching mechanism for spindle orientation and nuclear migration into the bud. J. Cell Biol. *139*, 985–994.

Thompson, J.D., Higgins, D.G., and Gibson, T.J. (1994). CLUSTAL W: improving the sensitivity of progressive multiple sequence alignment through sequence weighting, position-specific gap penalties and weight matrix choice. Nucleic Acids Res. *22*, 4673–4680.

Tirnauer, J.S., O'Toole, E., Berrueta, L., Bierer, B.E., and Pellman, D. (1999). Yeast Bim1p promotes the G1-specific dynamics of microtubules. J. Cell Biol. *145*, 993–1007.

Trusca, D., Scott, S., Thompson, C., and Bramhill, D. (1998). Bacterial SOS checkpoint protein SulA inhibits polymerization of purified FtsZ cell division protein. J. Bacteriol. *180*, 3946–3953.

Winston, F., Dollard, C., and Ricupero-Hovasse, S.L. (1995). Construction of a set of convenient *Saccharomyces cerevisiae* strains that are isogenic to S288C. Yeast *11*, 53–55.